Design of Longitudinal Members To Vehicle: Enhances The Energy Absorption of Thin Walled Structure Under Dynamic Load

Samer F. , Jamal O. Sameer, Abdulbasit Abdullah

Abstract— the present paper describes the behaviour of the thin wall rectangular tube cross- sections, subjected to dynamic compression load. We examine the reaction of the tube of various thicknesses and diameters, subjected to direct and oblique loading.

The study investigates the behaviour of the rectangular tube, with ellipse, circular and square shape triggers, and with various weight of hollow foam. The choice of the best design of tube parameter is based on the multi criteria decision making (MCDM) method. The examined parameters are the crush force efficiency, the peak force, and the energy absorption in case of direct and oblique loading. The rectangular tube is made of mild steel A36. Under direct load, with the usage of hollow aluminium foam, we can obtain 50% improvement f energy absorption and 84.6% of CFE. The enhancement under oblique load is 15.7% and 40.4% respectively. The aim of using thinner tube and hollow aluminium foam is to keep the final design the lowest possible weight, to improve the CFE and the energy absorber capacities in order to attain higher passenger safety.

Index Terms— dynamic compression, thin wall, energy absorption, direct and oblique loading, aluminum foam

I. INTRODUCTION

Recently the metallic foams have been significantly developed and this has opened new opportunities in the impact engineering. Properties, like high energy absorption capability at very light weight, high specific rigidity, constant distortion mode, and good adaptation to the distortion, etc. provide the necessary features for their application [1, 2].

Due to the promising properties of these materials, thin-walled structures with cellular or foamed filler materials under impact load, in the frontal longitudinal structures, have become subject of further researches [3–9]. The energy absorption capability of the metallic foam materials have been approved by the studies.

The complete numerical, and experimental research of Hanssen et al. [10–14] on the foamed filled thin-walled aluminium columns under direct load, contributed to the better understanding of the aluminium foam materials. The

results confirmed that the usage of foam-filler material considerably increases not only the energy absorption capability of the thin wall structures, but also the crush force. Hanssen et al. [14] solved a mass minimization question of the foam material properties, including the energy absorption capability, the force, and the stability of the aluminium columns of squared shape. They displayed – making use of a graphical analysis- the manifestation of the various crashworthiness dimensions.

Song et al. [15] similarly proved the relation between the usage of foam-filler materials in the thin-walled structure and its increased energy absorption capability. The results confirm that the filler materials and the geometry of the tube need to be taken simultaneously in consideration in order to detect the ideal design.

Chen [16] based empirical studies also on the mass minimization in order to investigate the crashworthiness features of the foam-filled tubes subjected to huge twisting rotational load. Afterwards Chen et al. [17] – with the help of the curve fitting technique - investigated the bending crush, in order to find the lowest possible weight with the required energy absorption capabilities and bending stiffness restrains. The main purpose of the research of Nariman-Zadeh et al. [18], was to obtain –with the usage of a multi objective genetic algorithm- the lowest possible weight, and in the same time the highest possible energy absorption capacities.

Zarei and Kroger [19,20] also used the multi-design optimization (MDO) for the geometric constraints of foam-filled tubes, as base of their experimental examination. The various researches focused mainly on the improvement of the experiential models of the foam-filled structures and their crashworthiness properties, while haven't been given attention to their design optimization. Moreover, Nariman-Zadeh et al. [18] denoted that the above mentioned design optimization should be processed in a multi objective framework, focusing on the effect of the various crashworthiness indicators on each other.

The purpose of the current study is to optimize the rectangular, aluminium foam filled thin-walled tube in case of for single and multiple crashworthiness indicators, and to improve their crashworthiness capabilities.

II. DESIGN METHODOLOGY

The study examines the behaviour of the cross sectional, thin wall, rectangular mild steel profile. The profile is long 350mm, thick 1, 1.2, 1.3 and 2mm, with various perimeters of 200 mm, 300 mm and 400 mm. As a first step, we survey the
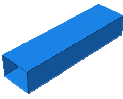
crashworthiness properties of the cross sectional profiles, and this is followed by the research of their improvement possibilities and the choice of the optimal design.

The rectangular profile of various weights is filled with hollow aluminium foam of 540kg/m3 density, and is subjected to direct and oblique (30 degrees) impact load. The simulation is based on an impact mass of the 25% of the total weight of the vehicle; with an initial speed of 54km/hr. Table 1 illustrates the various profiles.

**Table 1:** Geometry and dimensions of profiles used in the current study

Profile	Specimen ID	Perimeter mm	Length mm	Major Dimension mm	Thickness mm	Shape
Rectangular	R-200 R-300 R-400	300	350	60×40 90×60 112×74	1 1.2 1.3 2	

A. Force max and Peak load

The maximum force means the supreme impact, and the deformation that the members of the passenger car can absorb, maintaining the passenger cabin safe. The goal to achieve is to have vehicle members able to absorb the low-energy and low-velocity mass loads without constant deformation of the structure [21].

B. Energy Absorption

In Figure 1 the load-displacement curve illustrates the design of the energy absorption (EA) and its calculation.
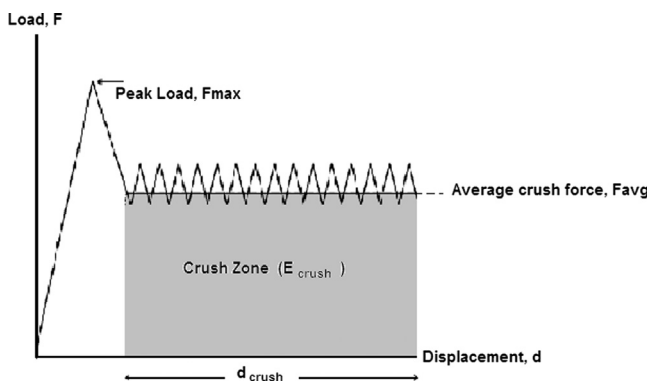
Fig .1. Force displacement characteristics [40]

$$EA = \int_0^{\delta b} P.d\delta \qquad (1)$$

P stands for the direct crush force; δ is for the deformation length of the crush, like in the calculation (1).

$$EA = \int_0^{\delta b} P.d\delta = P_m(\delta b - \delta i) \qquad (2)$$

P_m is stands for the crushing load; δi for the original length of the crushing specimen. The ideal energy absorption –once reached it- should maintain the maximum force for the whole length of the deformation.

C. Crush Force Efficiency, CFE

The crush force efficiency (CFE) is the main crushing force (P mean) divided by the peak crushing load (P peak) as follows.

$$CFE = \frac{P_{mean}}{P_{peak}} \qquad (3)$$

Based on the crash force efficiency (CFE) we can estimate the energy absorption capacities [22]. The value of CFE is computed by dividing the average value of force with the load- displacement curve on the peak force at the moment of the impact [23]. The goal is to keep the CFE at a high value, as its low value would mean high peak force and decreased passenger safety. The CFE indicates the effectiveness of the passenger car's structure, in case of an impact [24]. The required high CFE and low peak load values can be obtained by using the trigger mechanism [25] or by the usage of a thicker wall of the tube.

III. DYNAMIC ANALYSIS

The tests in the current study are performed by the software of ABAQUS/Explicit version 6.10, as finite element method, to simulate the profile's performance of the energy absorber members of the longitudinal frontal members of the vehicle in case of direct, and oblique dynamic load.

The software program is appropriate to simulate various procedures of computational fluid dynamics (CFD) or standard/ electrical model and in the same time it saves time, energy, and investment comparing to the implicit methods. It has the same abilities with the implicit methods in order to simulate identical circumstances of high speed dynamic, and impact load [26], and this makes it suitable to examine the effects of direct and oblique loads, and of the energy absorption capacity.

A. Finite Element Modeling

The below equation can be used in order to locate a point in a continuum:

$$\sigma_{ij} + f_i = \rho \ddot{X}_i \qquad (4)$$

or

σ_{ij} stands for the stress, ρ f the density, f_i for the body force and $\ddot{x}_i$ for the acceleration. Eq. (13) can be utilized in case of simulated work by the usage of the divergence theorem:

$$\int_V \rho \ddot{X}_i \delta X_i dV + \int_V \sigma_{ij} \delta X_{i,j} \, dV - \int_V \rho f_i \delta X_i \, dV - \int_{S^2} t_i \delta X_i \, dS = 0 \qquad (5)$$

In terms of the matrix form:

$$\sum_{i=1}^n \left\{ \int_v \rho N^t \, Nadv + \int_v B^t \sigma dv - \int_v \rho N^t bdv - \int_A N^t FdA + \int_S N^t F_c ds \right\}^i = 0 \qquad (6)$$

In the equitation n stands for the sum of components, σ for the stress column vector, N for the interpolation matrix, a for the nodal acceleration column vector, B for the strain matrix, b for the body load column vector, and F for the applied traction load (in case is applicable).
A more common explanation of this is shown below:

$$[M]\left[\frac{d^2u}{dt^2}\right] + [C]\left[\frac{du}{dt}\right] + [K]\{U\} = [F(t)] \qquad (7)$$

M stands for the mass matrix, C for the damping matrix and K for the stiffness matrix. The calculation of the displacements is followed by the computation of contact forces, internal and kinetic energies, and plastic strains. In case of nonlinear dynamic issues, like the impact, is desired to have explicit finite element software providing central difference method. The explicit method is able to separate the total length of time in minor time periods, called time steps or increments. The dynamic equilibrium calculations (see Eq. 1) are explained and the variables are defined at $(t+\Delta t)$ based on the information of their values at time t.
The explicit methods provide the data at time period n+1 based on the preceding time period (n) and without depending on the present time period, contrary to the implicit methods, where the time period n+1 is depends on the preceding, plus the present time period (n). In the current research, (FE) models of empty and foam filled tubes has been used by the non-linear FE code ABAQUS Explicit, in order to forecast the behaviour of the thin wall structures in case of falling impinging mass. The thin wall tube was modelled by the usage of 4 node shell continuum (S4R) elements and with 5 integration points alongside the thickness direction of the element. The foam was modelled using 8-noded continuum elements with the reduced integration techniques, in order to evade the volumetric locking, combined with the hourglass control, in order to evade artificial zero energy distortion. The size of the shells and foam elements is 5 mm, to guarantee an adequate mesh density to observe the distortion procedure. The "general contact algorithm" was chosen to simulate contact interaction among the components, and to evade interpenetration of the tube wall. The computational time of the current algorithm is less intensive. Connections among the empty and foam filled tube wall are modelled as finite sliding penalty based contact algorithm with contact pairs and hard contact. The rate of the friction coefficient for the surfaces is 0.2 [29, 30, and 32]. The striker, with impact velocity of 15 m/s (56 km/h), and compactor load of 275 kg, is modelled as a rigid body, having one translational displacement, while the rest of the translational and rotations degree are stable (Fig. 2).
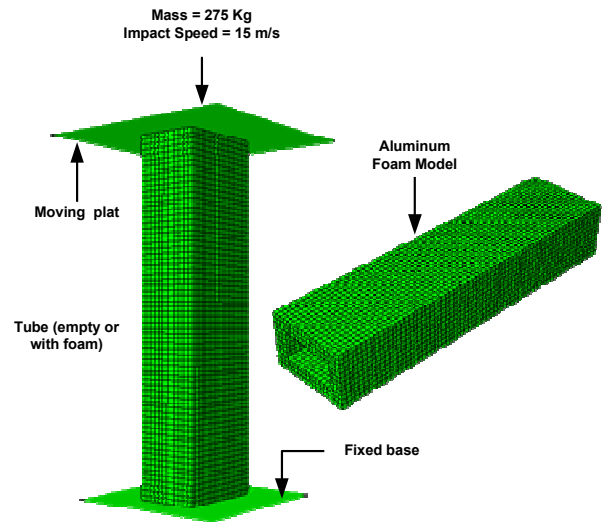

Fig.2. Design of frontal longitudinal members

The impact velocity is based on the New Car Assessment Program (NCAP) by the National Highway Traffic Safety Administration (NHTSA), with a mass of 25% of a vehicle (1100 kg). All the energy absorbing tubes are of A36 steel material, which is supposed to absorb the kinetic energy of 275 kg mass, as in natural conditions the supreme energy absorbed by two tubes is minor than 50% [30]. The classification of the A36 steel is based on the constitutive isotropic hardening model of Johnson–Cook, which considers the ratio of the strain effects and hardening, and is appropriate in cases with a big range of strain rate variety and temperature changes produced by the thermal softening [33]. The above features are shown in Eq. (3) [34]:

$$\sigma_T = \left[A + B\left(\varepsilon_{eff}^p\right)^N\right]\left[1 + C \ln \frac{\dot{\varepsilon}_{eff}^p}{\dot{\varepsilon}_0}\right]\left[1 - \left(\frac{T - T_0}{T_{melt} - T_0}\right)^M\right] \qquad (8)$$

σ_T stands for the flow stress in dynamic circumstances, ε_{eff}^P for the effects of the plastic strain, $\dot{\varepsilon}_{eff}^P$ for the effective plastic strain rate, A, B, N, M and C for the physical constraints and T_{melt} for the melting temperature, while T_0 for the alteration temperature. The typical temperature of it is 293-297 °K [33,35]. Table 3 shows the constraints of Johnson–Cook [35]. The options of crushable aluminium foam and its hardening possibilities in the usage of ABAQUS/Explicit software, are used in order to examine the plastic performance of the aluminium foam, follow the model of Dehspande and Fleck [36]. The yield condition of the model in question is as follows:

$$F = \hat{\sigma} - y \le 0 \qquad (9)$$

Where

$$\hat{\sigma}^2 = \frac{1}{[1 + (\alpha/3)^2]}\left[\sigma_e^2 + \alpha\sigma_m^2\right] \qquad (10)$$

Table 2: Mechanical properties of steel A36 material [26]

Factors	Value	Details
A	146.7 MPa	Material factor
B	896.9 MPa	Material factor
N	0.32	Coefficient of the strain power
C	0.033	Material factor
M	0.323	Power coefficient's temperature
ε^o	1.0 s−1	Reference strain value
ρ	7850 kg/m3	Material density
T_m	1773 K	Temperature of melting
Cp	486 J/kg-1K	Specific heat

σ_e stands for the effective von Mises stress, σ_m for the mean stress, and Y for the yield strength [37]. α stands for the form of the yield surface, and is a task of v_p, standing for the contraction's plastic constant, which is the rate of the plastic poisons of the aluminium foam material, with a presumed zero value [38, 39] as follows:

$$\alpha^2 = \frac{2(1-2\upsilon_p)}{9(1+\upsilon_p)} \quad (11)$$

In order to compute the strain hardening, the below calculation is integrated into the software:

$$Y = \sigma_p + \gamma\frac{\hat{\varepsilon}}{\varepsilon D} + \alpha_2 \ln\left[\frac{1}{1-(\hat{\varepsilon}/\varepsilon D)^\beta}\right] \quad (12)$$

σ_p, stands for the plateau stress, α_2, γ, ε_D and β represent the material property constants, while $\hat{\varepsilon}$ stands for the effective strain. ε_D, standing for the densification strain, can be computed as below:

$$\varepsilon_D = \frac{9+\alpha^2}{3\alpha^2}\ln\left(\frac{\rho_f}{\rho_{fo}}\right) \quad (13)$$

ρf stands for the foam density, and ρf_0 for the base material's density [32,33]. The specifications of foam filler materials of the dynamic model are illustrated in Table 4[38].

Table 3: Specific specifications of the aluminium foam material [36]

ρf (kg/m3)	σ_p(MPa)	α	α2 (MPa)	β	γ	ε_D
540	12.56	2.12	1544	3.68	1	1.6206

B. Interaction, Boundary Conditions and Loading

During the experimentation one end of the rectangular profile is fixed to the rigid body (plate) by tied constraint, in order to allow only a linear movement lengthwise the displacement direction. The rotating motion of the nodes on the rectangular profile is allowed. The role of the rigid bodies as plates is to ease the contact simulation. One of the rigid bodies is fixed in order to allow only the axial movement of the compactor body. The mass is applied on one of the reference points in the centre of one moving plate, with defined velocity and mass compactor. The role of the reference point, located in the

edge of the tube and the fixed plate, is to record the response. Step time with appropriate dynamic load, explicit action, and time period, which depends on the mesh dimension, and on the control and element structure, are specified by the program. The extended time interval requires more time to show the result and needs to have high CPU competency. The software ABAQUS/Explicit registers the interaction between all parts of the structure, like the contact between the walls and the aluminium foam, fixed plate, and the pofile. The interaction is concluded once the contact surface is specified and the "penalty" of the friction coefficient is assigned. During the experimentation, the rectangular tube is fixed from both ends to the rigid body, in order to obtain their movement like one body. The mesh extension of the rectangular tube, having deformation length during the crush, was specified at 5mm size [27], [28].

IV. RESULT AND DISCUSSION

Tables 4 and 5 show the results of the investigation. The detailed description follows in the next subsections.

Table 4: Result of crashworthiness factors in case of rectangular model with various parameters (direct load) at length deformation of 200 mm

Indictors	Direct Load R- 200			Direct Load R- 300			Direct Load R- 400		
	P max	CFE	Energy	P max	CFE	Energy	P max	CFE	Energy
1.0 mm	85.6	0.37	6.3	129	0.27	7	171	0.2	6.9
1.2 mm	103	0.41	8.6	155	0.32	9.95	206	0.23	9.6
1.3 mm	111	0.46	10.4	168	0.33	11.3	223	0.24	11
2 mm	182	0.54	20	267	0.38	20.9	357	0.32	23.6

Table 5: Result of crashworthiness factors in case of rectangular model with various parameters (oblique load) at length deformation of 200 mm

Indictors	Oblique Load R- 200			Oblique Load R- 300			Oblique Load R- 400		
	P max	CFE	Energy	P max	CFE	Energy	P max	CFE	Energy
1.0 mm	60.4	0.43	5.1	80	0.32	5.14	95.5	0.26	4.8
1.2 mm	73	0.49	7.1	96.7	0.36	7	118	0.3	7
1.3 mm	79	0.52	8.2	106	0.39	8.2	128	0.32	8.1
2 mm	124	0.72	17.8	163	0.52	16.9	195	0.43	16.7

A.   force displacement feature of different perimeter and thickness profile.

Figures 3 and 4 show the force displacement diagrams of the profile with 300 mm of perimeter, and the reaction of the different geometric profiles evoked by the direct and oblique load. Table 2 and 3 illustrate three types of perimeters (200 mm, 300 mm and 400 mm) and three different thicknesses (1, 1.2, 1.3, and 2 mm respectively). Based on the results, the quantity of the absorbed energy is significantly higher in case if direct load. This is caused by the fact that the oblique load has the force of the axial compression and also of the bending mode, resulted by the progressive crush. The result of the force-displacement demonstrates that the various parameters don't have effect on the folding process during the crush of the rectangular tube, subjected to oblique and direct load. Both actions have same kind of results during the progressive collapse.

B.   Energy Absorption

Figures 5 and 6 show the energy absorption capacity of the rectangular profile with 200 mm of deformation length, and with different perimeters, subjected to various impact loads, and without concentrating on the time factor. As shown by the figures, in every impact condition, by increasing the perimeter, proportionally increases the energy absorption capacity of the tube. The specific energy absorption (SEA) capacity of the rectangular profile geometry R-200 is lowest, while of the rectangular profile with 300 mm in diameter is the highest among all the profiles. Tables 4 and 5 show the energy absorption capacity of profiles with various thicknesses and perimeters, in case of the oblique load of 30 degrees. Based on the results, the tubes subjected to oblique load, had reduced energy absorption with a difference of 15 – 55 %. The optimal perimeter and thickness of the tube need to be chosen based on the CFE, the energy absorption capabilities, fabrication process, and weight.
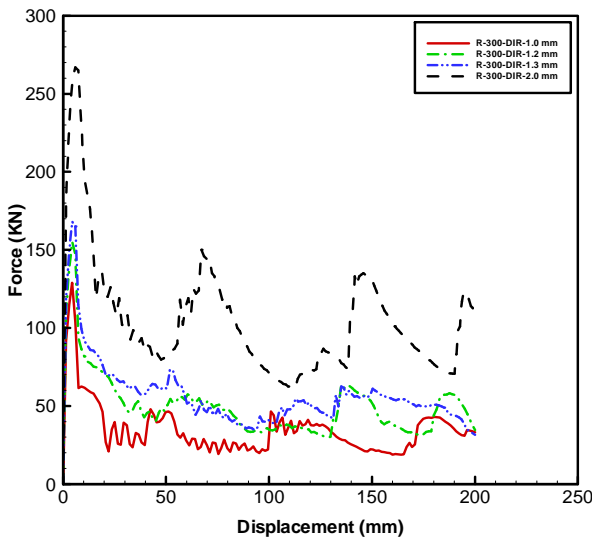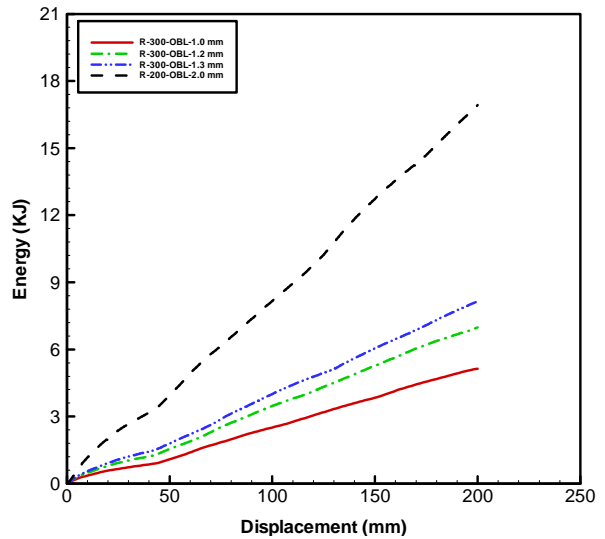

Fig.3. Force VS displacement for R-300 in case direct load
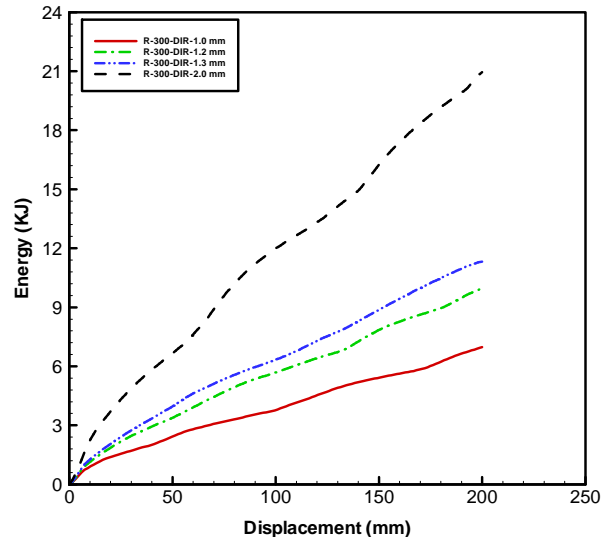
Fig.5. Energy VS displacement of R-300 in case of direct load
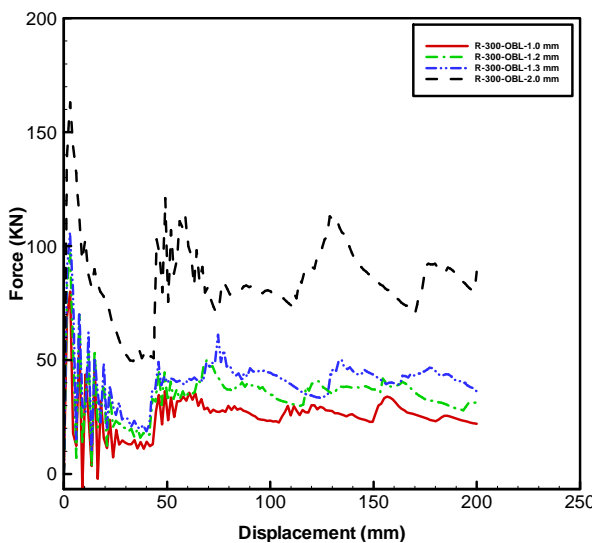
Fig.4. Fig.4. Force VS displacement for R-300 in case of oblique load

Fig.6. Energy VS displacement of R-300 in case of oblique load

C. Choise of the optimal profile

In this study the multi criteria decision making (MCDM) procedure is based on the complex proportional assessment method (COPRAS), which has the positive side of being convenient to handle. In case of the non-filled tubes, the 300 mm in diameter rectangular tube has the highest energy absorbing capability, followed by the 400 mm in diameter rectangular profile. In case of comparing the filled with the non-filled tubes, the rectangular profile of 300 mm in diameter filled with hollow aluminium foam has shown the best result in energy absorption capacity and crush force efficiency.

D. Effect of hollow foam on the energy absorption, peak force and CFE

The rectangular profile of 300 mm perimeter has been chosen for further examination regarding the wall thickness of the tube (1mm, 1.2mm, 1.3 mm and 2 mm), and the weight of the hollow aluminium foam filling (A of 0.955kg, B of 0.9074kg, C of 0.841kg, D of 0.756kg, and E of 0.652kg). Figures 7, 8, 9, 10, 11, 12, 13, 14, 15, 16, 17, and 18 illustrates how the use of various weight of hollow aluminium foam, and wall thickness increases the CFE and energy absorption. Thinner tube has been chosen in order to keep the final design as low as possible, while increasing the absorber capability and the CFE. As illustrated in Tables 8-9, in case of 1.3 mm wall thickness and 180 mm deformation length with hollow aluminium foam type (A), the enhancement of the energy absorption capacity and CFE raises from 10.5 KJ to 28.8 KJ, and 0.34 to 0.72 respectively in case of direct load, while the oblique load gives less positive results by an increase of 7.3 KJ to 17.7 KJ, and from 0.39 to 0.73 respectively.
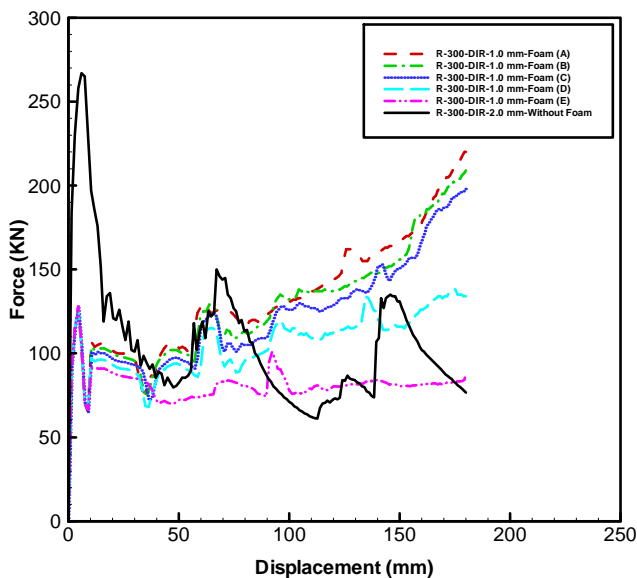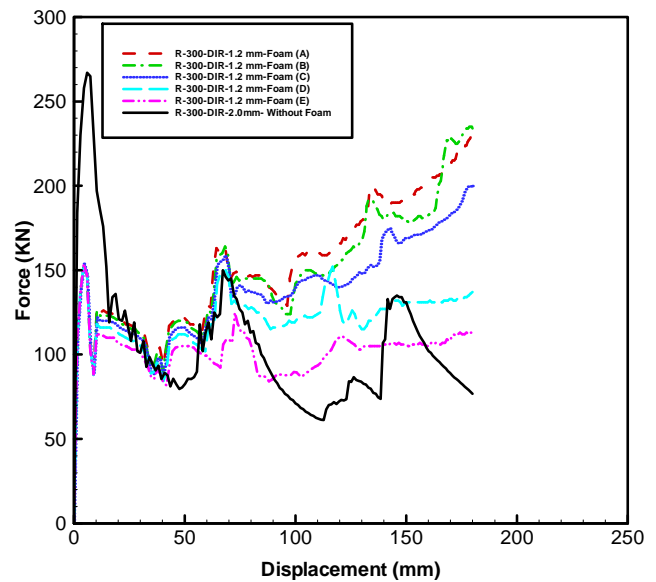

Fig.8. Force VS displacement of R-300 with different type of hollow aluminium foam, and wall thickness of 1.2 mm, in case of direct loads
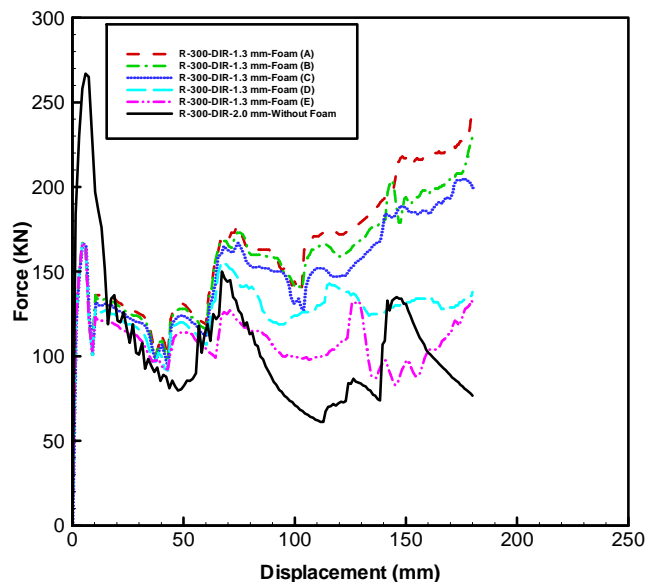

Fig.9. Force VS displacement of R-300 with different type of hollow aluminium foam, with wall thickness of 1.3 mm, in case of direct loads

Fig.7. Force VS displacement of R-300 with different types of hollow aluminium foam, and wall thickness of 1 mm, in case of direct load
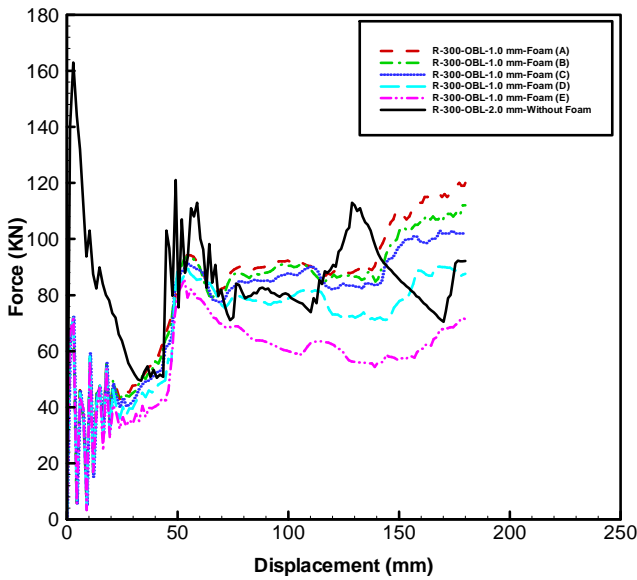
Fig.10. Force VS displacement of R-300 with different type of hollow aluminium foam, with wall thickness of 1 mm, in case of oblique load
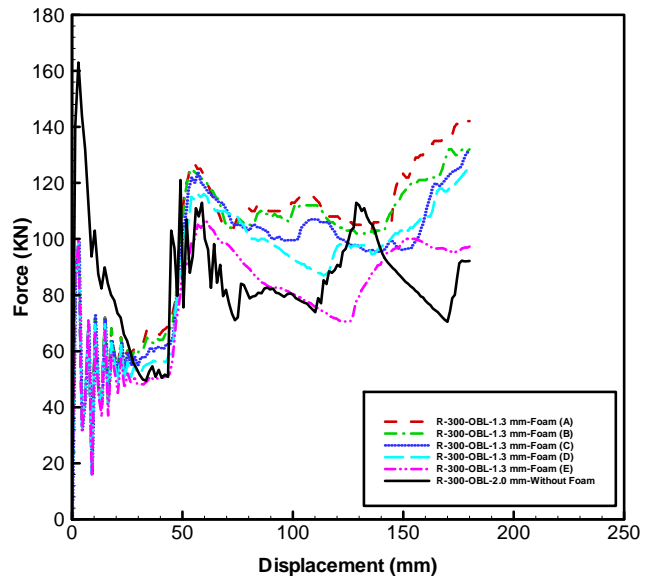

Fig.12. Force VS displacement of R-300 with different type of hollow aluminium foam, and thickness of 1.3 mm, in case of oblique load
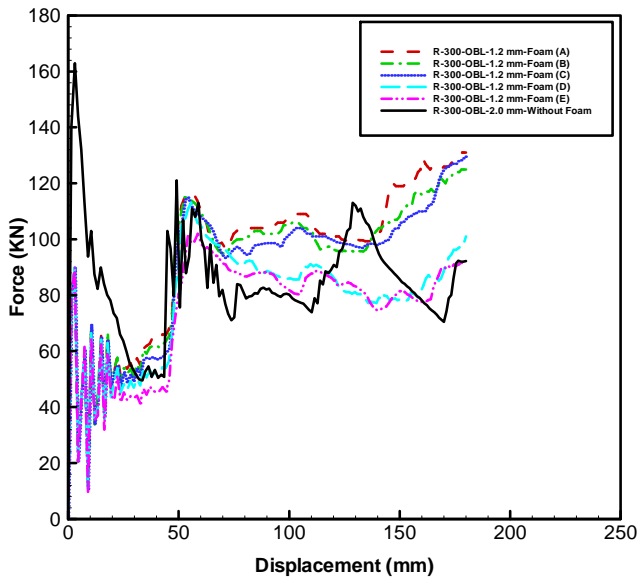

Fig.11. Force VS displacement of R-300 with different type of hollow aluminium foam, with wall thickness of 1.2 mm, in case of oblique load
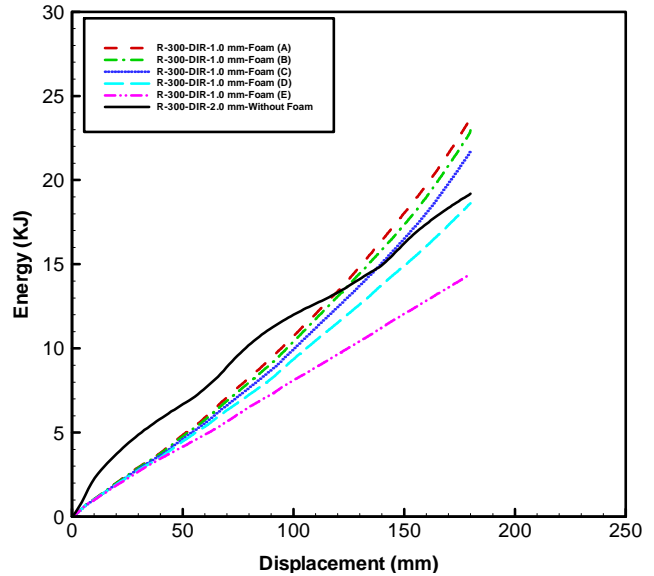

Fig.13. Energy VS displacement of R-300 with different type of hollow aluminium foam, with wall thickness of 1 mm, in case of direct load
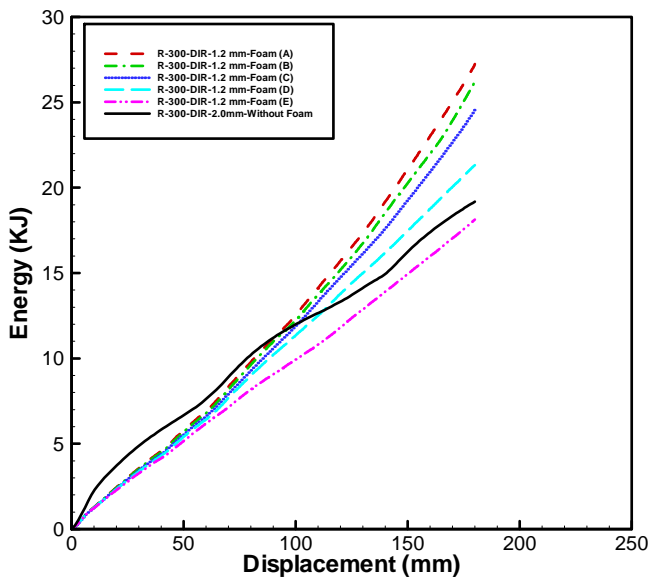
Fig.14. Energy VS displacement of R-300 with different type of hollow aluminium foam, and thickness of 1.2 mm, in case of direct load
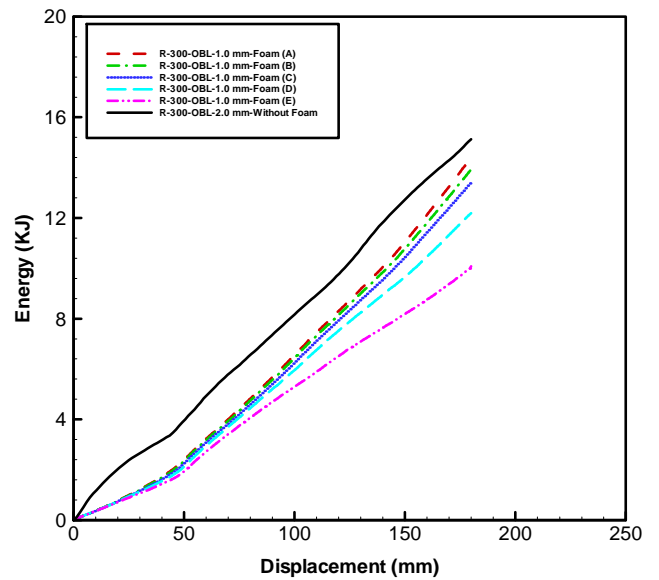

Fig.16. Energy VS displacement of R-300 with different type of hollow aluminium foam, with wall thickness of 1 mm, in case of oblique load
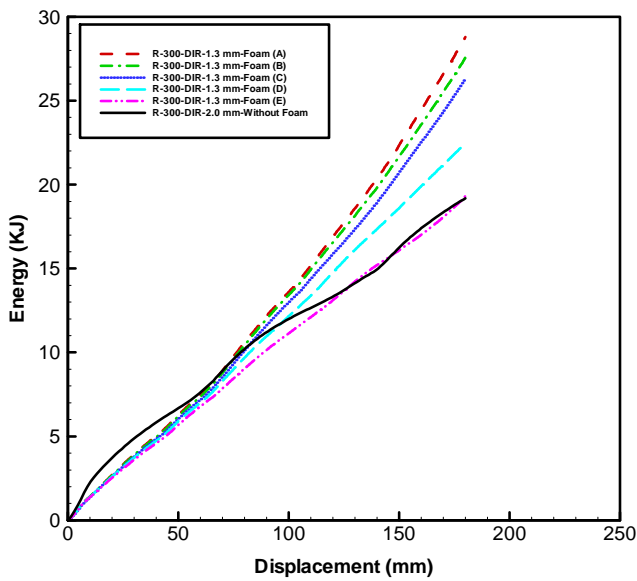

Fig.15. Energy VS displacement of R-300 with different type of hollow aluminium foam, with wall thickness of 1.3 mm, in case of direct load
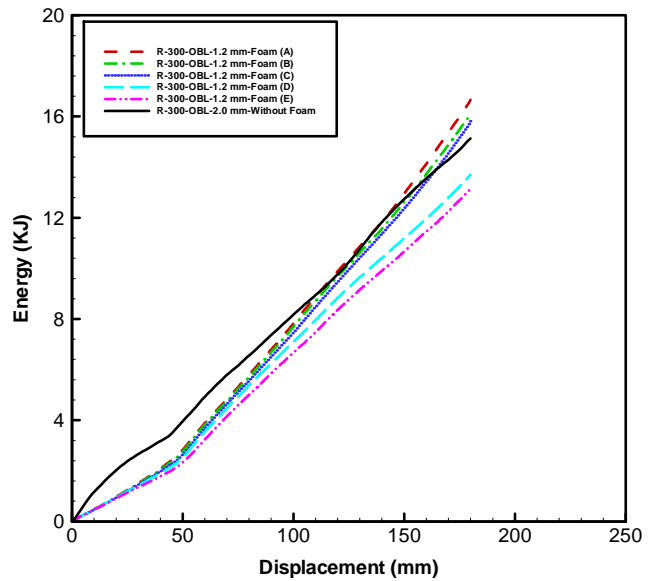

Fig.17. Energy VS displacement of R-300 with different type of hollow aluminium foam, with wall thickness of 1.2 mm, in case of oblique load
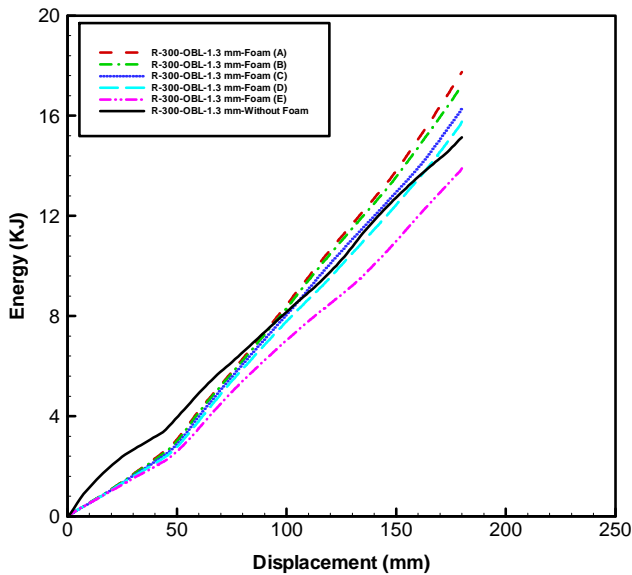
Fig.18. Energy VS displacement of R-300 with different type of hollow aluminium foam, with wall thickness of 1.3 mm, in case of oblique load

E. Effect of trigger mechanism

This study examines the effects of circular, ellipse, and square shaped triggers. The best results were given by the trigger with ellipse shape, and with the third type of distribution with three holes in each longitudinal side. From the reductions of 5, 7.5 10, 15 and 20%., the best result was given by the reduction of 10%, while from the positions of 10, 20, 30, 40, 50, 60 and 70 mm distance from the tube end, the best result was given by the position of 40 mm. As shown in Tables 6-7, the trigger mechanism had the best results in case of the rectangular profile with 2 mm wall thickness. The usage of the trigger mechanism increased the CFE by 7.3%, and the energy absorption by 8.4%. Figures 19, 20, 21, and 22, show the force and energy displacement function with the trigger mechanism.

Table 6: Energy absorption, peak force and CFE of profile R-300 with three different triggers under direct load at length deformation 200mm

| Profile-R-300 – Thickness 2 mm			
Criteria Type of Trigger	Peak force (KN)	CFE	Energy (KJ)
Without trigger	267	0.383	20.9
Circular trigger first dist.	265	0.4	21.69
Circular trigger second dist.	267	0.402	22
Circular trigger third dist.	266	0.404	22.21
Elliptical trigger first dist.	265	0.398	21.89
Elliptical trigger second dist.	266	0.405	22.11
Elliptical trigger third dist.	266	0.411	22.65
Square trigger first dist.	264	0.385	20.92
Square trigger second dist.	102	0.351	7.33
Square trigger third dist.	266	0.407	22.37
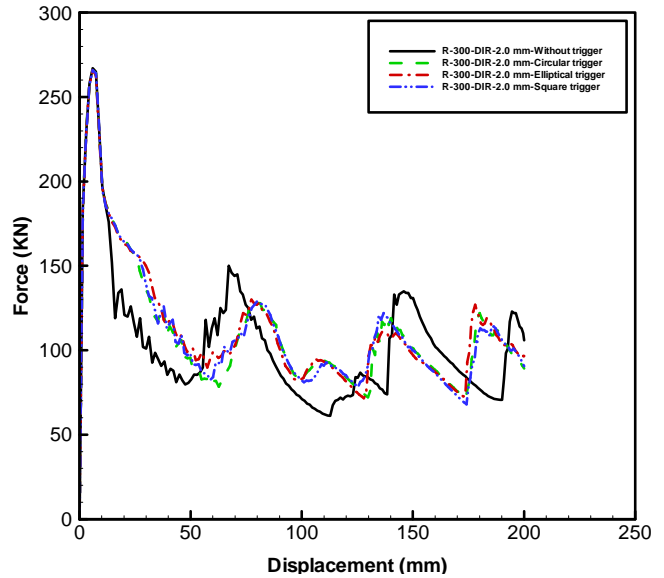
Fig.19. Force VS displacement of R-300 with the various triggers in case of direct load
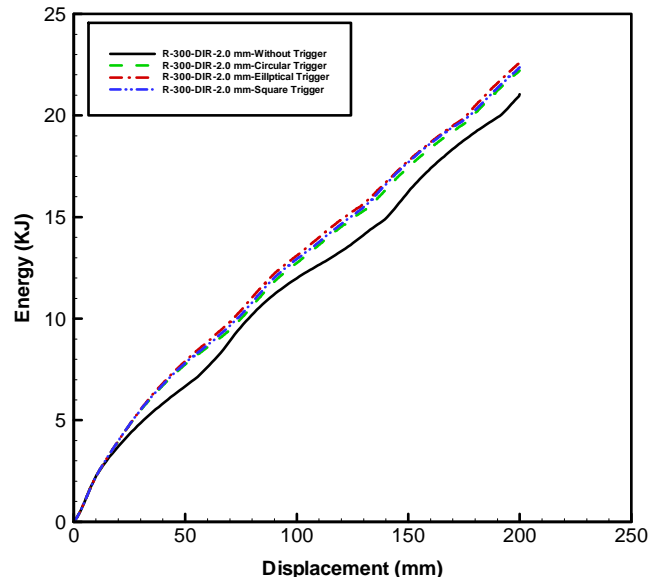

Fig.20. Energy VS displacement of R-300 with the various triggers in case of direct load
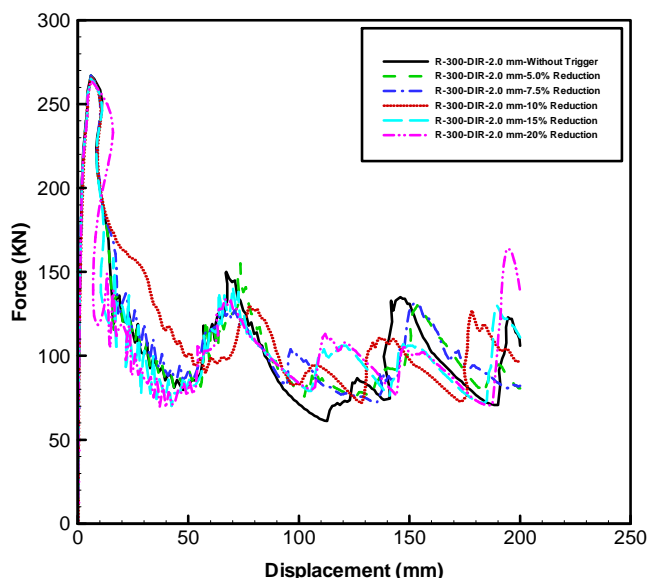
Fig.21. Force VS displacement of R-300 with the ellipse trigger at different reduction
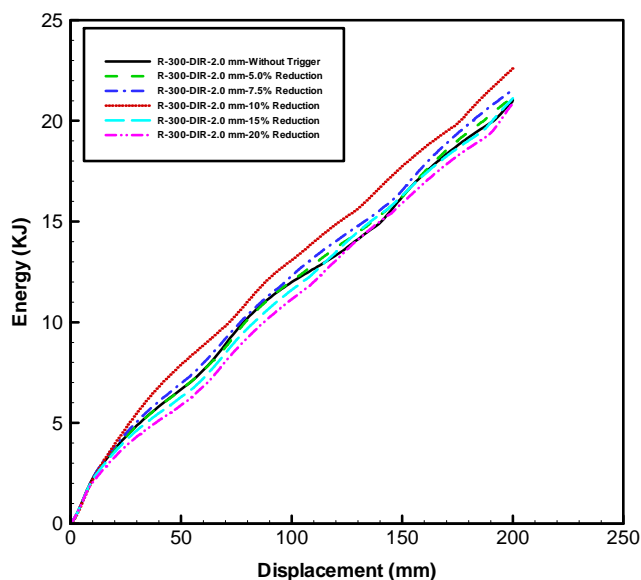

Fig.22. Energy VS displacement of R-300 with the ellipse trigger, at different reduction in case of direct load

Table 7: Energy absorption, peak force and CFE of profile R-300 with five different trigger reductions under direct load at length deformation of 200mm

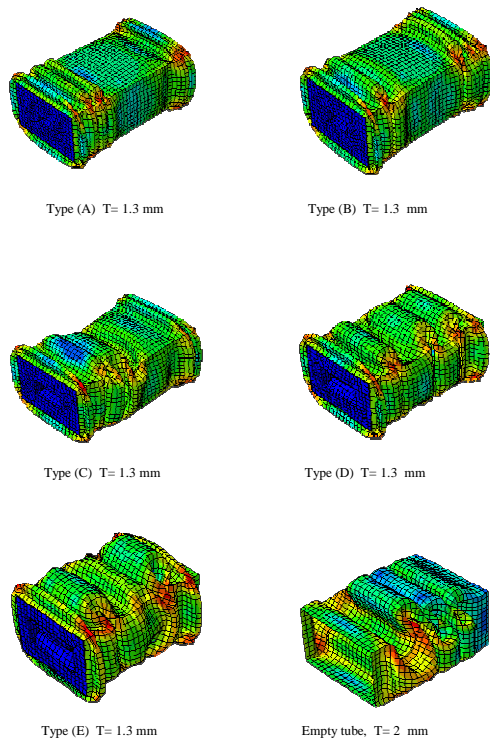| Profile-R-300 – Thickness 2 mm			
Criteria Trigger of type reduction	Peak force (KN)	CFE	Energy (KJ)
Without trigger	267	0.383	20.9
5% elliptical	267	0.387	21.19
7.5% elliptical	267	0.393	21.55
10% elliptical	266	0.411	22.65
15% elliptical	265	0.390	21.12
20% elliptical	264	0.391	20.86

V. CONCLUSION

The current study examined the oblique and the direct impact loads, and the effects of the impact on the rectangular tube of ductile material of mild steel (A36). The purpose of the research was to choose the best from the different rectangular profiles with various parameters. The next step was to observe the behaviour of the chosen profile, filled with aluminium foam of various weights, and to discover the best filling option in case of direct and impact load. Another examined option of increasing the energy absorption, and the CFE was the usage if the trigger mechanism.
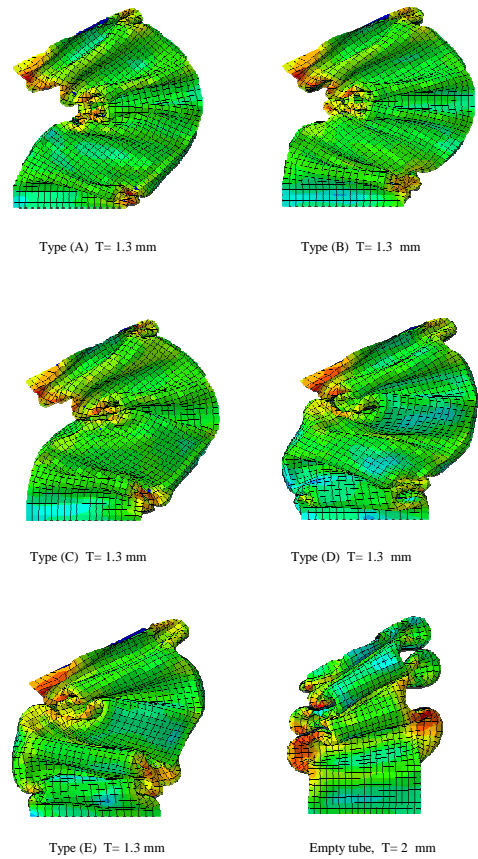
The dynamic simulation was conducted with the compact mass of 25% of the total weight (1100 kg) of the passenger car, with impact speed of 15 m/s, and with both direct, and oblique load on the rectangular profile. Based on the crash performance indicators, cost and manufacturing practicality, the optimal result of energy absorption capacity was given by the rectangular profile, thick 1.3 mm, and filled with hollow foam of type A (0.955kg), giving the values of 10.5 KJ for energy absorption, and 0.34 for CFE in case of direct load, while 7.3 KJ, and 0.39 in case of oblique load respectively. With 1.3 mm thick rectangular profile, the usage of hollow foam type A (0.955kg) filling had energy absorption value of 28.8 KJ, and CFE of 0.72 in case of direct load, and energy absorption value of 17.7 KJ, and CFE of 0.73 in case of oblique load.

The trigger mechanism with 2 mm thick rectangular tube enhanced the energy absorption capacities from 20.9 to 22.65 KJ and the CFE from 0.383 to 0.411. The best result is given by the trigger of ellipse shape with 10% reduction and 40 mm trigger position. To recapitulate, in case of direct load the increase of energy absorption was 50% and of CFE was 84.6%, while in case of oblique load the values were 15.7%, and 40.4%, respectively.

The best result has been given by the 1.3 mm thick rectangular profile filled with hollow aluminium foam type A (0.955 kg), and with the profile with ellipse shape triggers on the longitudinal side of the tube.These profiles can be recognized as a potential energy absorber candidates for crashworthiness applications.

Type (A) T= 1.3 mm   Type (B) T= 1.3 mm

Type (C) T= 1.3 mm   Type (D) T= 1.3 mm

Type (E) T= 1.3 mm   Empty tube, T= 2 mm

Fig.23. Crashing deformation of the longitudinal members, using different hollow aluminium foams, in case of steel material, and under oblique load

Type (A) T= 1.3 mm   Type (B) T= 1.3 mm

Type (C) T= 1.3 mm   Type (D) T= 1.3 mm

Type (E) T= 1.3 mm   Empty tube, T= 2 mm

Fig.24. Crashing deformation of the longitudinal members, using different hollow aluminium foams, in case of steel material, and under oblique load

Table 8: Effect of using different aluminium foam thicknesses, and tube thicknesses for R-300 subjected to direct load at length deformation of 180 mm.

Foam weight (Kg/mm2)		A (0.955 Kg)			B (0.9074 Kg)			C (0.841 Kg)			D (0.756 Kg)			E (0.652 Kg)		
Thickness	Criteria	P max (KN)	CFE	Energy (KJ)	P max (KN)	CFE	Energy (KJ)	P max (KN)	CFE	Energy (KJ)	P max (KN)	CFE	Energy (KJ)	P max (KN)	CFE	Energy (KJ)
1 mm		220	0.64	23.7	209	0.65	22.9	198	0.65	21.8	138	0.78	18.6	128	0.63	14.5
1.2 mm		230	0.71	27.3	235	0.67	26.2	200	0.73	24.6	154	0.79	21.3	154	0.66	18.1
1.3 mm		245	0.72	28.8	232	0.71	27.6	205	0.76	26.4	167	0.76	22.5	167	0.65	19.3
Empty tube 2 mm														267	0.39	19.2

Table 9: Effect of using different aluminium foam thicknesses, and tube thicknesses for R-300 subjected to oblique load at length deformation of 180 mm.

Foam weight (Kg/mm2)		A (0.955 Kg)			B (0.9074 Kg)			C (0.841 Kg)			D (0.756 Kg)			E (0.652 Kg)		
Thickness	Criteria	P max (KN)	CFE	Energy (KJ)	P max (KN)	CFE	Energy (KJ)	P max (KN)	CFE	Energy (KJ)	P max (KN)	CFE	Energy (KJ)	P max (KN)	CFE	Energy (KJ)
1 mm		120	0.7	14.5	112	0.73	14	103	0.76	13.4	90.1	0.78	12.2	85.8	0.67	10.1
1.2 mm		131	0.74	16.7	125	0.75	16.1	130	0.71	15.9	113	0.7	13.7	102	0.74	13.1
1.3 mm		142	0.73	17.7	132	0.76	17.2	131	0.72	16.3	126	0.73	15.8	107	0.75	13.9
Empty tube 2 mm														163	0.52	15.3

REFERENCES

[1]. Abramowicz, W., & Wierzbicki, T. (1988). Axial crushing of foam-filled columns. International Journal of Mechanical Sciences, 30(3), 263-271.

[2]. Abramowicz, W., & Wierzbicki, T. (1989). Axial crushing of multicorner sheet metal columns. Journal of Applied Mechanics, 56(1), 113-120.

[3]. Aktay, L., Toksoy, A. K., & Güden, M. (2006). Quasi-static axial crushing of extruded polystyrene foam-filled thin-walled aluminum tubes: experimental and numerical analysis. Materials & design, 27(7), 556-565.

[4]. Chen, W., & Wierzbicki, T. (2001). Relative merits of single-cell, multi-cell and foam-filled thin-walled structures in energy absorption. Thin-Walled Structures,39(4), 287-306.

[5]. Hanssen, A. G., Hopperstad, O. S., Langseth, M., & Ilstad, H. (2002). Validation of constitutive models applicable to aluminium foams. International journal of mechanical sciences, 44(2), 359-406.

[6]. Kavi, H., Toksoy, A. K., & Guden, M. (2006). Predicting energy absorption in a foam-filled thin-walled aluminum tube based on experimentally determined strengthening coefficient. Materials & design, 27(4), 263-269.

[7]. Kim, H. S. (2002). New extruded multi-cell aluminum profile for maximum crash energy absorption and weight efficiency. Thin-Walled Structures, 40(4), 311-327.

[8]. Santosa, S., & Wierzbicki, T. (1999). Effect of an ultralight metal filler on the bending collapse behavior of thin-walled prismatic columns. International Journal of Mechanical Sciences, 41(8), 995-1019.

[9]. Seitzberger, M., Rammerstorfer, F. G., Gradinger, R., Degischer, H. P., Blaimschein, M., & Walch, C. (2000). Experimental studies on the quasi-static axial crushing of steel columns filled with aluminium foam. International Journal of Solids and Structures, 37(30), 4125-4147.

[10]. Hanssen, A. G., Langseth, M., & Hopperstad, O. S. (1999). Static crushing of square aluminium extrusions with aluminium foam filler. International Journal of Mechanical Sciences, 41(8), 967-993.

[11]. Hanssen, A. G., Hopperstad, O. S., & Langseth, M. (2000). Bending of square aluminium extrusions with aluminium foam filler. Acta Mechanica, 142(1-4), 13-31.

[12]. Hanssen, A. G., Langseth, M., & Hopperstad, O. S. (2000). Static and dynamic crushing of square aluminium extrusions with aluminium foam filler.International Journal of Impact Engineering, 24(4), 347-383.

[13]. Hanssen, A. G., Hopperstad, O. S., & Langseth, M. (2001). Design of aluminium foam-filled crash boxes of square and circular cross-sections.International Journal of Crashworthiness, 6(2), 177-188.

[14]. Hanssen, A. G., Langseth, M., & Hopperstad, O. S. (2001). Optimum design for energy absorption of square aluminium columns with aluminium foam filler.International Journal of Mechanical Sciences, 43(1), 153-176.

[15]. Song, H. W., Fan, Z. J., Yu, G., Wang, Q. C., & Tobota, A. (2005). Partition energy absorption of axially crushed aluminum foam-filled hat sections.International Journal of Solids and Structures, 42(9), 2575-2600.

[16]. Chen, W. (2001). Optimisation for minimum weight of foam-filled tubes under large twisting rotation. International Journal of Crashworthiness, 6(2), 223-242.

[17]. Chen, W., Wierzbicki, T., & Santosa, S. (2002). Bending collapse of thin-walled beams with ultralight filler: numerical simulation and weight optimization. Acta mechanica, 153(3-4), 183-206.

[18]. Nariman-Zadeh, N., Darvizeh, A., & Jamali, A. (2006). Pareto optimization of energy absorption of square aluminium columns using multi-objective genetic algorithms. Proceedings of the Institution of Mechanical Engineers, Part B: Journal of Engineering Manufacture, 220(2), 213-224.

[19]. Zarei, H. R., & Kröger, M. (2007). Crashworthiness optimization of empty and filled aluminum crash boxes. International Journal of Crashworthiness, 12(3), 255-264.

[20]. Zarei, H., & Kröger, M. (2008). Optimum honeycomb filled crash absorber design. Materials & Design, 29(1), 193-204.

[21]. F. Tarlochan and Samer F. (2013). Design of thin wall structures for energy absorption applications: design for crash injuries mitigation using magnesium alloy. IJRET. 2 – (07)- 2319-1163.

[22]. Cheng, Q., Altenhof, W., & Li, L. (2006). Experimental investigations of the crush behavior of AA6061-T6 aluminum square tubes with different types of through-hole discontinuities. Thin-walled structures, 44 (4), 441-454.

[23]. Harte, A. M., Fleck, N. A., & Ashby, M. F. (2000). Energy absorption of foam-filled circular tubes with braided composite walls. European Journal of Mechanics-A/Solids, 19 (1), 31-50.

[24]. Olabi, A. G., Morris, E., Hashmi, M. S. J., & Gilchrist, M. D. (2008). Optimized design of nested circular tube energy absorbers under lateral impact loading. International Journal of Mechanical Sciences, 50 (1), 104-116.

[25]. Ahmad, Z., & Thambiratnam, D. P. (2009). Dynamic computer simulation and energy absorption of foam-filled conical tubes under axial impact loading. Computers & Structures, 87 (3), 186-197.

[26]. Nagel, G. (2005). Impact and energy absorption of straight and tapered rectangular tubes (Doctoral dissertation, Queensland University of Technology).

[27]. Nagel, G. M., & Thambiratnam, D. P. (2005). Computer simulation and energy absorption of tapered thin-walled rectangular tubes. Thin-Walled Structures, 43 (8), 1225-1242.

[28]. Witteman, W. J. (1999). Improved vehicle crashworthiness design by

control of the energy absorption for different collision situations: proefschrift. Technische Universiteit Eindhoven.

[29]. Dehghan-Manshadi, B., Mahmudi, H., Abedian, A., & Mahmudi, R. (2007). A novel method for materials selection in mechanical design: combination of non-linear normalization and a modified digital logic method. Materials & design,28(1), 8-15.

[30]. Olabi, A. G., Morris, E., Hashmi, M. S. J., & Gilchrist, M. D. (2008). Optimised design of nested circular tube energy absorbers under lateral impact loading.International Journal of Mechanical Sciences, 50(1), 104-116.

[31]. Witteman, W. J. (1999). Improved vehicle crashworthiness design by control of the energy absorption for different collision situations: proefschrift. Technische Universiteit Eindhoven.

[32]. Ahmad, Z., & Thambiratnam, D. P. (2009). Dynamic computer simulation and energy absorption of foam-filled conical tubes under axial impact loading.Computers & Structures, 87(3), 186-197.

[33]. Duan, C. Z., Dou, T., Cai, Y. J., & Li, Y. Y. (2011). Finite element simulation and experiment of chip formation process during high speed machining of AISI 1045 hardened steel. AMAE International Journal on Production and Industrial Engineering, 2(1).

[34]. Dean, J., Dunleavy, C. S., Brown, P. M., & Clyne, T. W. (2009). Energy absorption during projectile perforation of thin steel plates and the kinetic energy of ejected fragments. International journal of impact engineering, 36(10), 1250-1258.

[35]. Lacy, J. M., Shelley, J. K., Weathersby, J. H., Daehn, G. S., Johnson, J., & Taber, G. (2010, October). Optimization-based constitutive parameter identification from Sparse Taylor cylinder data. In Proceedings of the 81st shock and vibration symposium. Idaho National Laboratory, US.

[36]. Deshpande, V. S., & Fleck, N. A. (2000). Isotropic constitutive models for metallic foams. Journal of the Mechanics and Physics of Solids, 48(6), 1253-1283.

[37]. Shahbeyk, S., Petrinic, N., & Vafai, A. (2007). Numerical modelling of dynamically loaded metal foam-filled square columns. International journal of impact engineering, 34(3), 573-586.

[38]. Ahmad, Z., & Thambiratnam, D. P. (2009). Dynamic computer simulation and energy absorption of foam-filled conical tubes under axial impact loading.Computers & Structures, 87(3), 186-197.

[39]. Reyes, A., Hopperstad, O. S., Berstad, T., Hanssen, A. G., & Langseth, M. (2003). Constitutive modeling of aluminum foam including fracture and statistical variation of density. European Journal of Mechanics-A/Solids, 22(6), 815-835.

[40]. Tarlochan, F., Samer, F., Hamouda, A. M. S., Ramesh, S., & Khalid, K. (2013). Design of thin wall structures for energy absorption applications: Enhancement of crashworthiness due to axial and oblique impact forces. Thin-Walled Structures, 71, 7-17.

AUTHORS

Samer F. Was born in Iraq. He obtained his Bachelors in Mechanical Engineering and Master in Mechanical Engineering from Iraq. He obtained his PHD in Mechanical Engineering from UNITEN, Malaysia. He is a lecturer at College of Engineering, Alanbar University, Iraq.

Jamal O. Sameer was born in Iraq. He obtained his Bachelors in Mechanical Engineering from Iraq. He is currently pursuing his Master of Mechanical Engineering in the field of applied Mechanical Engineering at Universiti Tenaga Nasional (UNITEN), Kajang, Selangor, Malaysia.

Abdulbasit Abdullah was born in Iraq. He obtained his bachelors in General of Mechanical Engineering from Iraq. He is currently pursuing his Master of Mechanical Engineering in the field of applied Mechanical Engineering at Universiti Tenaga Nasional (UNITEN), Kajang, Selangor, Malaysia.